Paired-pulse depression of unitary quantal amplitude at single hippocampal synapses

Gong Chen*†, Nobutoshi C. Harata*, and Richard W. Tsien*‡

*Department of Molecular and Cellular Physiology, Beckman Center, Stanford University School of Medicine, Stanford, CA 94305; and †Department of Biology, Pennsylvania State University, University Park, PA 16802

Contributed by Richard W. Tsien, November 18, 2003

At central synapses, quantal size is generally regarded as fluctuating around a fixed mean with little change during short-term synaptic plasticity. We evoked quantal release by brief electric stimulation at single synapses visualized with FM 1–43 dye in hippocampal cultures. The majority of quantal events evoked at single synapses were monovesicular, based on examination of amplitude distribution of α-amino-3-hydroxy-5-methyl-4-isoxazolepropionic acid-receptor-mediated responses. Consistent with previous findings, the quantal size did not change during paired-pulse facilitation (PPF), supporting the notion that the evoked events were monoquantal. However, during paired-pulse depression (PPD), there was a significant decrease in unitary quantal size, which was not due to postsynaptic receptor desensitization. This asymmetry of quantal modulation during PPF and PPD was demonstrated at the same single synapse at different extracellular calcium concentrations. Our results indicate that PPF can be fully accounted for by an increase of release probability, whereas PPD may be caused by decreases in both release probability and quantal size. One possible explanation is that the release of a quantum of neurotransmitter from synaptic vesicles is not invariant but subject to rapid calcium-dependent modulation during short-term synaptic plasticity.

Short-term synaptic plasticity is important for synaptic communication within the brain and is classically assessed with "paired-pulse stimulation," two stimuli in close succession. There are various forms of paired-pulse modulation (PPM), typically attributed to different mechanisms. Paired-pulse facilitation (PPF) is generally explained as an increase of release probability (P_r) during the second stimulus, arising from prior accumulation of residual Ca^{2+} near active zones or a lingering effect of Ca^{2+} on a Ca^{2+} sensor (1, 2). In contrast, paired-pulse depression (PPD) comes in multiple forms (3) and is open to a much wider range of possible explanations: receptor desensitization can be important in some cases (4) but is in general excluded. Instead, PPD is thought to originate presynaptically in most systems, as reflected by decreased transmitter output (5, 6). Reduced presynaptic release is most often attributed to vesicular depletion (7–11), but evidence for additional presynaptic mechanisms independent of vesicular depletion has also been provided (12–16).

Deciphering PPM calls for a clear picture of quantal transmission at single synapses, but this is still under debate. Although general agreement has been reached about a lack of receptor saturation at excitatory synapses (17–19), controversy remains as to what generates variability in excitatory postsynaptic current (EPSC) size. One view is that single CNS synapses obey a "one-vesicle rule," whereby presynaptic release is somehow capped at no more than one vesicle per presynaptic spike (8, 20–23). The unitary evoked EPSC would then constitute a response to exocytosis of a single presynaptic vesicle, the evoked counterpart of a classical miniature EPSC (mEPSC), and variations in potency (8) might depend on the manner in which single vesicles release neurotransmitters. The other view, that multivesicular release freely occurs at single synapses (24, 25), implies that changes in potency would be dominated by variations in the number of vesicles released per trial.

Previous approaches to these issues have largely relied on minimal stimulation of putative single-input axons in slices, which leaves residual uncertainty about the number of synapses activated. In this study, putative single presynapses in hippocampal culture were visually identified and locally stimulated. We observed neurotransmission that satisfied stringent tests for univesicular release but that also showed a significant decrease in the size of unitary EPSCs with PPD. Thus, under certain conditions, the potency of unitary transmission can be subject to modulation.

Methods

Cell Culture. Autaptic hippocampal neurons were cultured by using a method modified from previous ones (26). Briefly, the hippocampal CA1–CA3 region was dissected out from postnatal 1- to 2-day-old rats. Tissues were trypsinized (5 mg/ml, 5–10 min) and dissociated by trituration. Cells were plated at a very low density (2,000–3,000 cells per cm^2) on microdots (100- to 500-μm diameter) of poly-D-lysine and collagen sprayed with micropipettes, to obtain isolated single autaptic neurons. The culture medium contained MEM, 5 g/liter glucose, 0.2 g/liter $NaHCO_3$, 100 mg/liter bovine transferrin, 2 mM glutamine, 25 mg/liter insulin, 10% FCS (HyClone), and 2% B-27 supplement (GIBCO). After 1 d in culture, serum was reduced to 5%, and glutamine was reduced to 0.5 mM. After 3–4 d in culture, cytosine-β-arabinofuranoside (4 μM) was added to the medium to stop proliferation of glial cells. The culture was maintained in a humidified incubator (5% CO_2 and 95% O_2) for 2–3 wk.

Electrophysiology. Whole-cell recordings were made on autaptic pyramidal neurons with an Axopatch-1C or Axopatch 200B amplifier (Axon Instruments, Foster City, CA). The recording chamber was continuously perfused with Tyrode solution (1 ml/min) containing 125 mM NaCl, 2 mM KCl, 1 or 3 mM $CaCl_2$, 3 or 1 mM $MgCl_2$, 30 mM glucose, and 25 mM Hepes (pH 7.3 with NaOH). The patch pipette (2.0–3.8 MΩ) solution contained 100 mM KCl, 10 mM NaCl, 10 mM Tris-phosphocreatine, 20 units/ml creatine phosphokinase, 4 mM MgATP, 3 mM Na_2GTP, 2 mM EGTA, and 30 mM Hepes (pH 7.3 with KOH). The series resistance was usually 8–20 MΩ and continuously monitored. If >30% change occurred, data were rejected. Data were digitized at 10 kHz, filtered at 2 kHz, and acquired/analyzed by using PCLAMP 8 software (Axon Instruments) and customized software written in LABVIEW (National Instruments, Austin, TX). Experiments were performed at room temperature (23–25°C).

Identification and Stimulation of Single Boutons. To identify a single bouton of an autaptic neuron, FM 1–43 (10 μM) was applied in 70 mM $[K^+]$ (plus 10 μM 6-cyano-7-nitroquinoxaline-2,3-dione and 50 μM D,L-2-amino-5-phosphopentanoic acid (D,L-AP5) to prevent activation of glutamate receptors) for 2 min and then washed off for >5 min (27, 28). Fluorescent images were taken with an inverted

Abbreviations: PPM, paired-pulse modulation; PPF, paired-pulse facilitation; PPD, paired-pulse depression; EPSC, excitatory postsynaptic current; mEPSC, miniature EPSC; CV, coefficient of variation; P_r, release probability; $[Ca^{2+}]_o$, external Ca^{2+}.

See Commentary on page 907.

‡To whom correspondence should be addressed. E-mail: rwtsien@stanford.edu.

Nikon Diaphot 200 microscope and acquired/analyzed with customized software written in LABVIEW. Isolated boutons, usually >7 μm from neighboring boutons, were selected for experiments. To obtain evoked release from a single bouton, a θ-tube stimulating electrode (≈2-μm tip diameter) containing bathing solution was placed very close to the selected bouton, and a brief current pulse (2–3 ms, 1–3 μA) between the barrels was applied with an Iso-Flex stimulator (AMPI, Jerusalem) (29). Tetrodotoxin (1 μM), D,L-AP5 (50 μM), and bicuculline (20 μM) were included in the bathing solution throughout the single-bouton experiments to prevent transmitter release from nonstimulated boutons and to isolate α-amino-3-hydroxy-5-methyl-4-isoxazolepropionic acid receptor responses. Each single synapse was subjected to 200–600 paired stimulations (50-ms interstimulus interval), repeated at 0.2–0.5 Hz. To minimize stimulus artifacts, traces containing failures were identified according to a template composed of the average of 10–20 traces with stimuli applied in the presence of 6-cyano-7-nitroquinoxaline-2,3-dione (10 μM). Each individual trace was subjected to subtraction of the average of 4–10 failure traces in its temporal proximity. Successful events were detected as signals exceeding a threshold three times the rms of baseline noise and phase-locked with the stimulation (within 3-ms range).

Results

Evoked Quantal Release at Single Synapses Visualized with FM 1–43. To test whether unitary quantal release can be modulated during short-term synaptic plasticity, it is advantageous to evoke quantal responses at visually identifiable single synapses. We used FM 1–43 to identify presynaptic boutons for electrophysiological analysis (Fig. 1*A*) (17, 27–30). We chose dye-stained puncta whose intensity was below average (Fig. 1*B*, downward arrow), generally avoiding the faintest puncta (which usually failed to support evoked responses) and the brightest ones (which might have been multiple boutons in close proximity). The boutons selected for recordings were also relatively isolated, being separated from their nearest neighbors by an average distance of 9.0 ± 0.6 μm (n = 14). Tetrodotoxin (1 μM) was included in the bathing solution to block action potentials. Individual nerve terminals were depolarized by application of brief current pulses between the barrels of a fine-tipped θ-pipette, positioned within 1–2 μm of the isolated bouton. If the θ-pipette was moved a few micrometers away from the selected bouton, the stimulating pulses were no longer able to evoke responses (Fig. 1*D*). Fig. 1*C* shows representative data obtained with whole-cell recording from the cell body. The arrows indicate the application of paired stimuli to the bouton (50-ms interval). The traces show examples of the four possible patterns (failure–failure, success–failure, etc.), along with a spontaneous mEPSC (Fig. 1*C*, *). When the first or second stimulus evoked an EPSC, it always appeared in a close temporal relationship with the stimulus. The release probabilities (P_r) for the first and second responses were 0.55 and 0.58 at this bouton. Amplitude distributions of the first and second EPSCs are shown in Fig. 1 *E* and *F*. Both histograms displayed only a single peak and were not significantly different from each other ($P > 0.5$, Kolmogorov–Smirnov test for all comparisons between amplitude distributions). The distributions were close to Gaussian in form, with similar median values (9.34 and 9.26 pA, respectively) and coefficients of variation (CV) (CV 0.33 and 0.44, respectively). The evoked EPSCs can be compared with a useful benchmark, the spontaneous mEPSCs from the same recording, which may originate from both stimulated and nonstimulated boutons and vary in quantal amplitudes (Fig. 1*G*). These were somewhat larger (median 12.70 pA) and more broadly distributed (CV 0.50) (Fig. 1*H*, $P < 0.01$ for both parameters). The set of findings in Fig. 1 *E–H* was in keeping with evoked monoquantal release.

It is instructive to compare this pattern with that found in other recordings where transmitter release was patently multiquantal (Fig. 1 *I–L*), as often found with focal stimulation of FM puncta whose fluorescent intensity was far above average (arrowhead in Fig. 1*B*). In this case, the median amplitude of the first EPSC (18.8 pA) was double that of the mEPSC (8.8 pA). Furthermore, the histograms of evoked EPSC amplitudes seemed to contain multiple peaks, unlike the mEPSC distribution. Evidently, the largest evoked events consisted of multiple quantal units, not just single quanta. This would be expected if the brightness of the punctum arose from a single large bouton with multiple release sites or from close proximity of multiple boutons, each with their own release sites. Whatever the morphological basis, the physiological characteristics clearly pointed to simultaneous release of multiple vesicles, leading us to set aside such recordings as unsuitable for the present analysis.

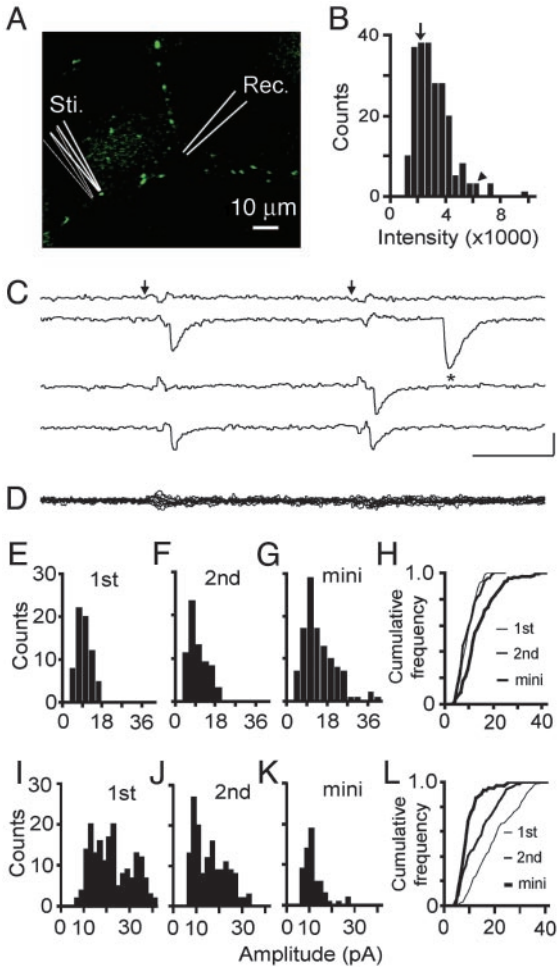

Fig. 1. Quantal release evoked from visualized single synapses. (*A*) Image showing presynaptic FM 1–43-stained boutons. Isolated boutons (usually >7 μm away from neighboring boutons) were selected for experiments. (*B*) Histogram of integrated intensities for FM 1–43-stained puncta. The arrow indicates the intensity of the bouton selected for stimulation in *A*, yielding the results in *C–H*. The arrowhead corresponds to the punctum used for *I–L*. (*C*) Evoked EPSCs from the isolated bouton, recorded in the presence of tetrodotoxin (1 μM) and 1 mM Ca^{2+}. The asterisk indicates a mEPSC. (*D*) Overlay of 10 traces showing no evoked response after θ-pipette had been moved laterally from the selected bouton (thin lines in *A*). (*E–G*) Amplitude distribution histograms for the first EPSC (*E*), second EPSC (*F*), and spontaneous mEPSCs (*G*). Failures were excluded in *E* and *F*. (*H*) Cumulative frequency plot illustrating that the evoked EPSCs (first and second) are smaller than the mEPSCs ($P < 0.01$, Kolmogorov–Smirnov test for all of the amplitude distribution comparisons), suggesting monoquantal release. (*I–K*) The amplitude distribution of the first, second, and spontaneous mEPSCs recorded from the large punctum denoted in *B* (arrow). (*L*) Cumulative frequency plot showing that the evoked EPSCs (first and second) are much larger than the mEPSCs ($P < 0.001$), consistent with multiquantal release.

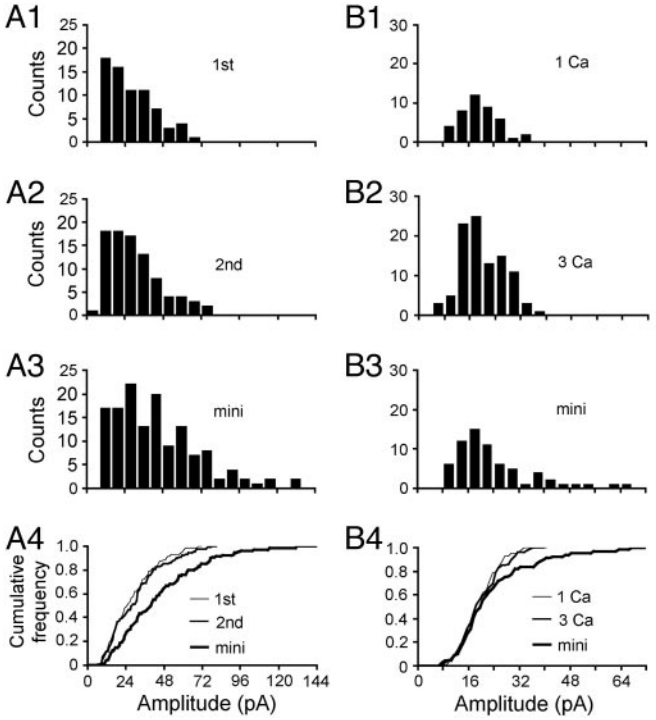

Fig. 2. Characteristics of monoquantal release at single synapses. (*A1–A3*) Amplitude distributions for the first EPSC, second EPSC, and mEPSC recorded in 1 mM Ca^{2+}/3 mM Mg^{2+}. (*A4*) Superimposed cumulative distributions illustrating the first and second EPSCs were not different ($P > 0.4$), but both were significantly smaller than the mEPSCs ($P < 0.001$). (*B1–B4*) Comparison between the quantal size evoked at 1 vs. 3 mM Ca^{2+} bath solution at one single synapse. No statistical difference between the quantal size evoked in 1 vs. 3 mM Ca^{2+} solution ($P > 0.9$), and both were not different from the mEPSCs ($P > 0.2$).

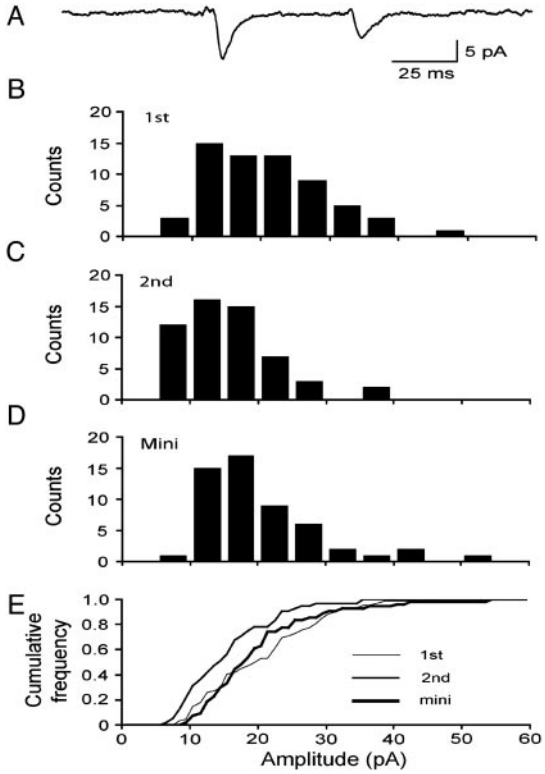

Fig. 3. Quantal size reduction during PPD. (*A*) Average of all traces (failures included) shows significant PPD (PPM = 0.55) in 3 mM Ca^{2+}/1 mM Mg^{2+}. (*B–D*) Amplitude distributions for the first EPSC (median = 20.0 pA), second EPSC (14.4 pA), and mEPSC (18.2 pA). (*E*) Superimposed cumulative distributions demonstrating the mEPSC and the first EPSCs were no different ($P > 0.14$), but the second EPSCs were smaller than either the first EPSCs ($P < 0.01$) or the mEPSCs ($P < 0.02$).

Monovesicular Release of Evoked EPSCs at Single Synapses. To date, it is still controversial to what extent synaptic transmission at excitatory hippocampal synapses conforms to a one-vesicle rule (8, 21–25, 31, 32). We found that transmission at visually identified single synapses generally showed properties consistent with monovesicular behavior. Fig. 2 *A1–A4* illustrates a single synapse recording made in 1 mM Ca^{2+}/3 mM Mg^{2+} (overall PPF = $EPSC2_{avg}/EPSC1_{avg} = 1.6$, failures included in averages). Although more skewed than in Fig. 1 *E–H*, the amplitude distributions of the successful responses to the first and second stimuli (Fig. 2 *A1–A2*, failures excluded) were very similar, with medians of 25.6 and 28.2 pA ($P > 0.4$), both smaller than that of the minis (Fig. 2*A3*). The differences ($P < 0.001$) are highlighted in cumulative histograms (Fig. 2*A4*). The overall PPF was largely accounted for by a greater incidence of successes during the second trial ($P_r = 0.61$) than during the first ($P_r = 0.42$). This result is consistent with previous findings at putative single hippocampal synapses where PPF has been accounted for by a change of P_r (8, 21–23).

In addition to the PPF test, we further tested the monovesicular rule by varying the bath calcium concentration (Fig. 2 *B1–B4*) (22). With 1 or 3 mM external Ca^{2+} ($[Ca^{2+}]_o$), the EPSC amplitude distribution was almost identical ($median_{1Ca} = 18.9$ pA; $median_{3Ca} = 18.7$ pA; $P > 0.9$), despite a sizable increase in P_r ($P_{r1Ca} = 0.17$; $P_{r3Ca} = 0.40$). Neither of the median amplitudes was statistically different from those of mEPSCs (median of miniamplitudes = 20.4 pA, $P > 0.2$).

To summarize results obtained in 12 single synapse recordings, the median sizes of evoked quantal EPSCs and spontaneous mEPSCs were not significantly different ($P > 0.1$ by paired t test). Both varied widely from one recording to the next (9.1–34.1 pA for evoked EPSCs, 10.8–37.8 pA for mEPSCs), but the average median values were quite similar (19.0 ± 2.2 and 22.6 ± 2.9 pA, respectively). The CV values for evoked EPSC sizes averaged 0.43 ± 0.02, significantly less than the CV of corresponding mEPSCs, 0.57 ± 0.03 (paired t test, $P < 0.003$) (30). Likewise, the skew of evoked EPSC histograms averaged 0.72 ± 0.07, significantly less than that of mEPSCs, 1.68 ± 0.13 (paired t test, $P < 0.001$). These comparisons indicated that the evoked EPSCs were as close to monoquantal as spontaneous mEPSCs.

Quantal Size Decreases During PPD. In contrast to the recordings made in 1 mM Ca^{2+}/3 mM Mg^{2+}, which usually resulted in PPF, recordings made in 3 mM Ca^{2+}/1 mM Mg^{2+} often showed significant PPD. This form of depression is not to be confused with the refractoriness found at <20 ms intervals, called "lateral inhibition" (8, 33), which completely dissipates within the 50-ms interval studied here. Quantal analysis of the evoked EPSCs during PPD revealed a surprising decrease of unitary quantal size. Fig. 3 illustrates results from a synapse with prominent PPD overall (Fig. 3*A*; $EPSC2_{avg}/EPSC1_{avg} = 0.55$, failures included). With failures excluded, the quantal size of the second EPSCs (Fig. 3*C*; $median_{2nd} = 14.4$ pA) was significantly smaller than the first EPSCs (Fig. 3*B*; $median_{1st} = 20.0$ pA; $P < 0.01$). The median value of mEPSCs was 18.2 pA (Fig. 3*D*), not statistically different from the first EPSCs ($P > 0.14$) but larger than the second EPSCs ($P < 0.02$). As seen in Fig. 3*E*, the cumulative histograms of first and second EPSCs and mEPSCs display CV values in the range of 0.40–0.45, typical of the single synapse recordings. These results suggest that, although both first and second responses arose from monoquantal release, the unitary amplitude was significantly reduced in association with PPD. Along with the 28% decrease of median quantal size during PPD, P_r also decreased from 0.76 to 0.67, a reduction

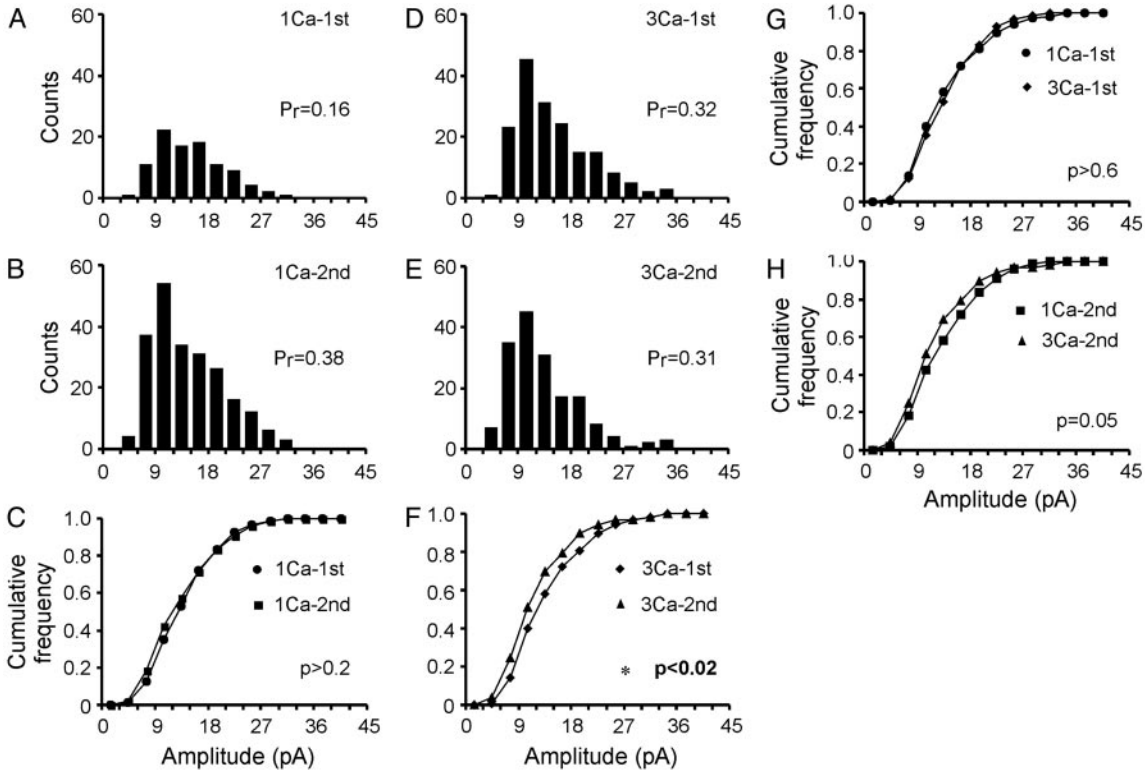

Fig. 4. Asymmetry of quantal modulation during PPF and PPD at the same synapse. (*A* and *B*) Amplitude distribution of the first and second EPSCs evoked at 1 mM Ca^{2+} bath solution. (*C*) Overlay of the cumulative plots showing no statistical difference between the first and second EPSCs ($P > 0.2$), indicating monoquantal. (*D* and *E*) Amplitude distribution of the first and second EPSCs recorded in 3 mM Ca^{2+} bath solution. The same synapse as for *A* and *B*. (*F*) Overlay of the cumulative plots showing that the second EPSCs were significantly smaller than the first ones ($P < 0.02$). (*G*) Overlay of the cumulative plots of the first EPSCs in 1 and 3 mM Ca^{2+} solution ($P > 0.6$), supporting monovesicular release. (*H*) Overlay of the cumulative plots of the second EPSCs in 1 and 3 mM Ca^{2+} solution ($P = 0.05$).

of 12% from the first to second trial. Thus, the overall PPD was generated by changes in both quantal size and P_r.

Quantal Modulation During PPF and PPD at the Same Synapse. Our results suggest that the modulation of quantal size displayed an asymmetry: quantal size did not change during PPF but decreased during PPD. To test this further, we examined the quantal modulation during both PPF and PPD, studied at the same synapse. Fig. 4 illustrates an experiment in which the overall PPM was 2.6 at 1 mM Ca^{2+} and 0.8 at 3 mM Ca^{2+}. At 1 mM $[Ca^{2+}]_o$ (Fig. 4 *A–C*), the quantal sizes of the first and second EPSCs (Fig. 4 *A* and *B*) did not differ (Fig. 4*C*, $P > 0.2$), whereas the P_r increased ($P_{r1st\text{-}1Ca} = 0.16$; $P_{r2nd\text{-}1Ca} = 0.38$). In contrast, at 3 mM $[Ca^{2+}]_o$ (Fig. 4 *D–F*), the quantal size for the second EPSCs was significantly smaller than the first EPSCs ($P < 0.02$), whereas P_r hardly decreased ($P_{r1st\text{-}3Ca} = 0.32$; $P_{r2nd\text{-}3Ca} = 0.31$). These results confirmed that quantal size was differently modulated during PPF and PPD. The first EPSCs in 1 and 3 mM $[Ca^{2+}]_o$ (Fig. 4 *A* and *D*) were not different in size (Fig. 4*G*, $P > 0.6$), even though P_r increased 2-fold, providing further assurance that the evoked transmission at single synapses was monoquantal.

***P*r and Quantal Size Both Contribute to PPM.** Fig. 5 shows pooled results for the quantitative contributions of changes in quantal size and P_r to PPM. Ratios of second and first trial values for quantal size (q_2/q_1) and P_r (P_{r2}/P_{r1}) were plotted against the overall PPM

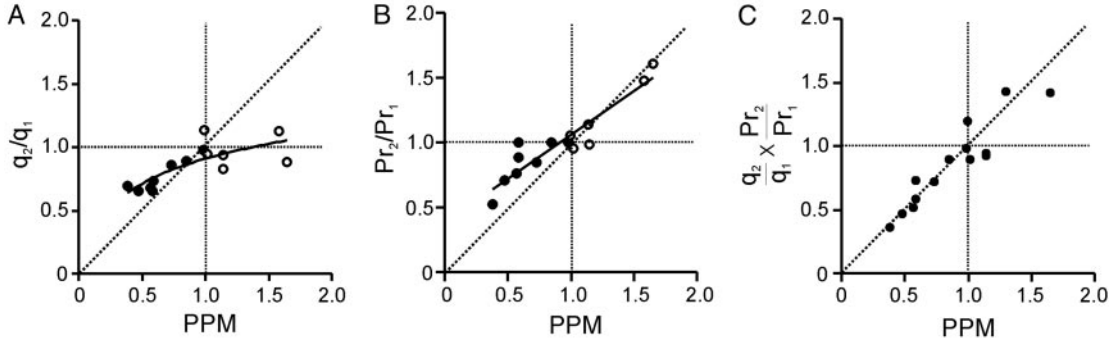

Fig. 5. Both quantal size and P_r change during PPM. (*A*) Plot of quantal size (q) changes vs. the overall PPM (PPM = $EPSC2_{avg}/EPSC1_{avg}$, all sweeps). Data were fitted by $y = 0.29$ Ln $(x) + 0.91$ (solid line). Also shown is the line of unity (dashed diagonal line). Note that quantal size change is more significant in the PPD regime (PPM <1). Filled circle, 3 mM Ca^{2+}; open circle, 1 mM Ca^{2+}. (*B*) Plot of P_r changes vs. the overall PPM. Note that the P_r changed in both PPF (PPM >1) and PPD regimes. Data were fitted by $y = 0.68x + 0.38$ (solid line). (*C*) Multiplication of the raw data points in *A* and *B* gave a product (solid circles) very close to the line of unity.

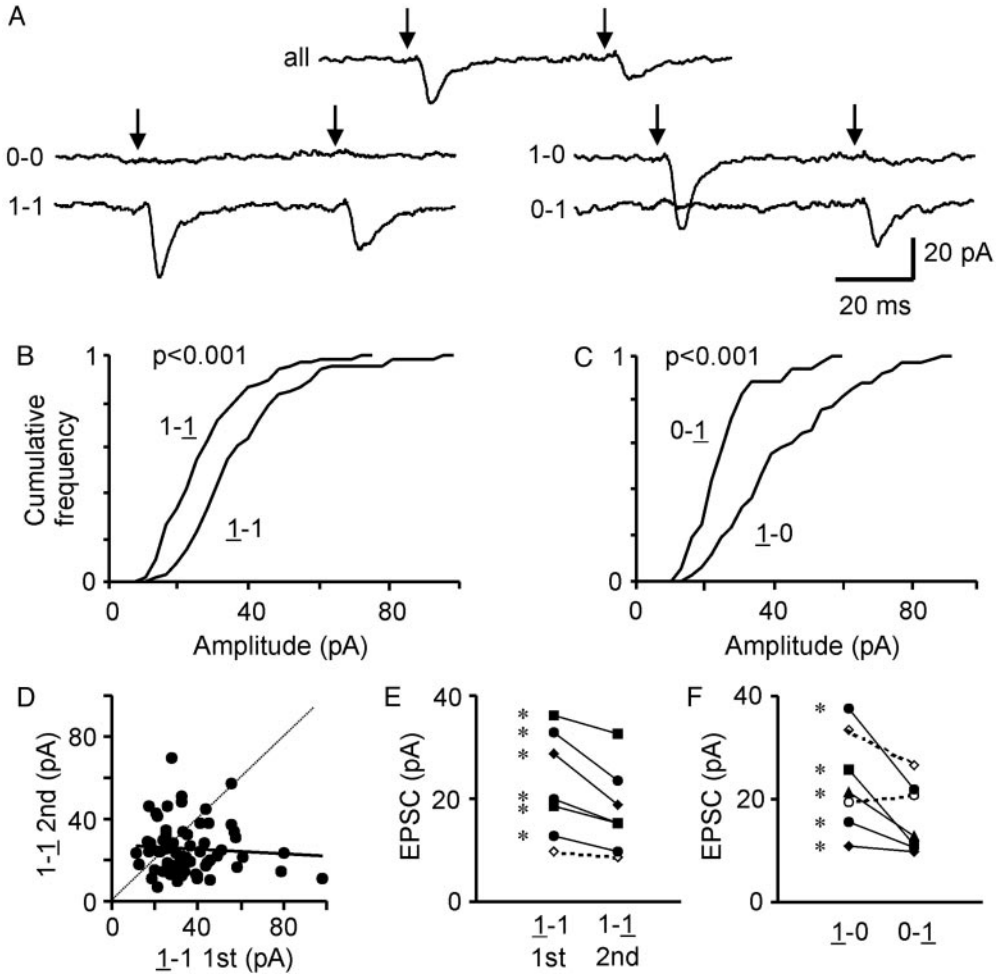

Fig. 6. Analysis of contingent effects on unitary quantal size. (*A*) Representative recordings from a single synapse showing prominent PPD (PPM = 0.48), taken with 3 mM Ca^{2+}/1 mM Mg^{2+}. Records are averages from every trace (all), traces with failures on both trials (0-0), traces with successes on both trials (1-1), and other combinations (1-0 and 0-1). (*B*) Cumulative distributions of the first and second EPSC amplitudes in the 1-1 case. The distribution of second EPSCs (1-*1*, median = 23.4 pA) was significantly smaller than that of the first (*1*-1, median = 32.5 pA) ($P < 0.001$). (*C*) Cumulative distributions showing the second EPSC amplitude in the 0-1 case (median = 21.7 pA) was significantly smaller than the first EPSC amplitude in the 1-0 case (median = 37.2 pA) ($P < 0.001$). (*D*) The plot of the second (1-*1*) response vs. the first (*1*-1) response in every 1-1 trial. Most points fell below the line of unity (dotted), indicating that the second response was generally smaller than the first one. Linear regression showed no correlation between the first and the second response ($r = -0.08$, $P > 0.5$). (*E*) Pooled data demonstrating that six of seven experiments showed a significant reduction in quantal size for the second response (*); one pair lacked statistical significance (dashed line). (*F*) Comparison between the median of the first EPSC amplitude in the 1-0 case and the second EPSC amplitude in 0-1 case. Five of seven experiments showed a significantly smaller quantal size for the response in the 0-1 case than the response in the 1-0 case (asterisk; exceptions are indicated by dashed lines).

(Fig. 5 *A* and *B*). The change in quantal size was prominent and consistent for PPD (PPM <1) but was not detected with PPF (PPM >1). In contrast, the P_r changed significantly in both PPF and PPD regimes (Fig. 5*B*). The observed change in P_r was not sufficient to account for the overall PPD, indicated by data points consistently deviating from the line of unity (dashed diagonal, Fig. 5*B*). However, when the ratio of quantal sizes (Fig. 5*A*) was multiplied by the ratio of P_rs (Fig. 5*B*) for each synapse, the product came close to the 45° line. It is clear that alterations in both quantal size and P_r contributed to the overall PPD.

PPD in the Absence of Postsynaptic Receptor Desensitization or Vesicular Depletion. A classical explanation of a diminished second response is desensitization of postsynaptic receptors after a successful first response. To test this and other scenarios, we looked closely at how changes in quantal amplitude depended on the immediate previous history as illustrated in Fig. 6. Responses to paired stimulation were subdivided into the four possible patterns: 0-0, 1-0, 0-1, and 1-1, where 0 or 1 denotes failure or success, and averages of each of the groups were examined (Fig. 6*A*). The recording solution contained 3 mM Ca^{2+}/1 mM Mg^{2+}, and the P_r for the first and second responses was 0.55 and 0.39, respectively. As a check, we verified that the first response amplitude in the 1-1 case (32.5 pA) and the first response amplitude in the 1-0 case (37.2 pA) were not significantly different ($P > 0.08$). We also determined that the second response in 1-1 case (23.4 pA) was similar to the second response in the 0-1 case (21.7 pA) ($P > 0.5$). Evidently, the size of the second response was independent of whether neurotransmitter release had occurred during the first trial, in agreement with Hjelmstad *et al.* (33). In the same vein, the 1-1 records showed no correlation between the first (*1*-1) and second (1-*1*) responses (Fig. 6*D*). This indicated that any desensitization arising from the first response had completely disappeared by the time of the second stimulus (33).

Interestingly, in the 1-1 case, the median value of the second EPSC was 23.4 pA, significantly smaller than the median of the first EPSC, 32.5 pA (Fig. 6*B*, $P < 0.001$). This finding was representative of six of seven cells in which 1-1 trials were sufficiently numerous to warrant analysis (Fig. 6*E*). The reduction of the second response

was not just an after-effect of vesicular release evoked by the first stimulus (Fig. 6 *C* and *F*). In the 0-1 case, the median of the successful EPSCs was 21.7 pA, significantly smaller than the median EPSC size of 37.2 pA in the 1-0 group (Fig. 6*C*, $P < 0.001$). This finding was representative of five of seven recordings (Fig. 6*F*). The same conclusion holds if the second responses in either the 1-*1* or 0-*1* case are compared with the first responses pooled together from both the *1*-1 and *1*-0 case ($P < 0.001$). Thus, a first stimulus that failed to release neurotransmitter could nonetheless reduce the size of the response to a second stimulus. The appearance of this difference seemed related to the use of external solution with relatively high Ca^{2+} (3 mM), conditions under which PPD was strong. No such effect was observed in recordings with 1 mM Ca^{2+}/3 mM Mg^{2+}, in which case the medians of EPSC2 and EPSC1 were not significantly different (six of six experiments).

Discussion

We evoked synaptic transmission from a single excitatory nerve terminal by focal electric stimulation in a cultured neuronal system for direct visualization of dye-labeled presynaptic boutons. This approach has the advantage that single presynaptic boutons can be selected for features such as their degree of isolation from their neighbors. The application of focal depolarization in the presence of tetrodotoxin eliminated concerns about conduction failure in axons and axon branches and uncertainties about the number of discrete synaptic connections in play.

Our results provided a test of the one-vesicle rule at single visually identified excitatory synapses. Consistent with published studies using minimal axonal stimulation in brain slices (8, 22, 23), we found no significant change in synaptic potency under conditions in which P_r was strongly increased (PPF or elevated $[Ca^{2+}]/[Mg^{2+}]$ ratio; Figs. 2 and 4). Both skewed and Gaussian amplitude distributions were able to pass appropriate tests. Our findings are consistent with the prior proposal that, in at least a subset of excitatory central nerve terminals, the evoked quantal output of a single terminal can be essentially restricted to one vesicle per presynaptic depolarization (8, 22, 23). Two qualifications must be noted. First, the statistical test for significant differences between potency under low and high P_r conditions does not allow us to exclude a small number of two-vesicle release events. Thus, we cannot certify that the one-vesicle rule applied absolutely in a particular experiment, but only that multivesicular release hardly ever took place. Second, our experiments provided evidence consistent with the existence of multivesicular release (Fig. 1 *I–L*), particularly at very brightly stained puncta. This observation may help in reconciling apparently conflicting views (34) on univesicular (8, 22, 23) vs. multivesicular release (24, 25, 31, 32). The bright puncta likely correspond to large boutons, presynaptic counterparts of the big postsynaptic spines (35) that would be favored in providing strong optical signals for quantal analysis (24, 25). In contrast, purely electrophysiological recordings using distant stimulation would select for synapses obeying the one-vesicle rule (3).

Unlike the constant quantal amplitude (potency) during PPF, we found that quantal size significantly decreased during PPD, even at single synapses conforming rigorously to the one-vesicle rule (Fig. 4). In pooled data, the quantitative contributions to PPD of lowered P_r and reduced quantal size were roughly equal (Fig. 5). This enlarges the set of possible mechanisms for PPD, which already includes conduction failure (15), Ca^{2+} channel failure (3), release site refractoriness (8), decreased P_r (5, 16, 36), and postsynaptic desensitization (4, 36).

Our conditional analysis of successes and failures (Fig. 6) helps narrow the range of possible mechanisms. The successful second trial responses are significantly smaller than the successful first trial responses even in cases where the first response was a failure. This argues against scenarios that require the completion of first trial vesicle release (e.g., presynaptic vesicle depletion and postsynaptic desensitization) as wholly adequate explanations. Our work is in keeping with previous evidence against significant residual desensitization at intervals of 30–70 ms in hippocampal slices (33). Our evidence for a mechanism beyond that of depletion is consistent with recent studies at other central synapses (13, 14). Evidently, the inhibitory influence of the first stimulation can arise from a signal upstream of vesicle fusion, possibly Ca^{2+} entry (3), rather than vesicular release per se.

Other possible scenarios remain open as ways of accounting for the diminution of quantal size during PPD. One might imagine that the second stimulus evokes fusion of a smaller vesicle or one less completely filled with neurotransmitter, although there is no evidence to indicate that vesicles are sorted by size or glutamate content. Alternatively, release-ready vesicles might differ in how favorably they are aligned with postsynaptic receptors (37); the first event might correspond to glutamate release at the optimal location and the second event to exocytosis at a less optimal position such as the synapse periphery. Finally, quantal size during the second trial might be attenuated by a fusion pore opening that is smaller, briefer, or more gradual in onset than that seen on first stimulation. How this might come about could be related to the observation that quantal size changes were seen specifically with PPD induced by high $[Ca^{2+}]_o$ (22). Ca^{2+}-dependent regulation of fusion pores has been demonstrated in neuroendocrine cells (38). Adaptive inhibition of exocytosis by photolytic elevation of intracellular Ca^{2+} concentration has been shown at the squid giant synapse (12). An unsuccessful first stimulus might leave the release machinery in two very different conditions, depending on the strength of Ca^{2+} entry: an available state that follows simple failure to trigger fusion or an adapted or inactivated state in which the efficiency of fusion is impaired. This would account for the restricted appearance of quantal modulation in PPD but not PPF.

This work was supported by the National Institute of Mental Health (R.W.T.), the Mathers Charitable Trust (R.W.T.), a National Research Service Award from the National Institutes of Health (to G.C.), and the Pennsylvania State University Life Science Consortium Innovative Biotechnology Research Fund (G.C.).

1. Zucker, R. S. (1999) *Curr. Opin. Neurobiol.* **9,** 305–313.
2. Neher, E. (1998) *Neuron* **20,** 389–399.
3. Dobrunz, L. E., Huang, E. P. & Stevens, C. F. (1997) *Proc. Natl. Acad. Sci. USA* **94,** 14843–14847.
4. Chen, C., Blitz, D. M. & Regehr, W. G. (2002) *Neuron* **33,** 779–788.
5. Silver, R. A., Momiyama, A. & Cull-Candy, S. G. (1998) *J. Physiol.* **510,** 881–902.
6. Hashimoto, K. & Kano, M. (1998) *J. Physiol.* **506,** 391–405.
7. Thies, R. E. (1965) *J. Neurophysiol.* **28,** 427–442.
8. Stevens, C. F. & Wang, Y. Y. (1995) *Neuron* **14,** 795–802.
9. Dobrunz, L. E. & Stevens, C. F. (1997) *Neuron* **18,** 995–1008.
10. Wang, L. Y. & Kaczmarek, L. K. (1998) *Nature* **394,** 384–388.
11. Dittman, J. S., Kreitzer, A. C. & Regehr, W. G. (2000) *J. Neurosci.* **20,** 1374–1385.
12. Hsu, S. F., Augustine, G. J. & Jackson, M. B. (1996) *Neuron* **17,** 501–512.
13. Bellingham, M. C. & Walmsley, B. (1999) *Neuron* **23,** 159–170.
14. Waldeck, R. F., Pereda, A. & Faber, D. S. (2000) *J. Neurosci.* **20,** 5312–5320.
15. Brody, D. L. & Yue, D. T. (2000) *J. Neurosci.* **20,** 2480–2494.
16. Wu, L. G. & Borst, J. G. (1999) *Neuron* **23,** 821–832.
17. Liu, G., Choi, S. & Tsien, R. W. (1999) *Neuron* **22,** 395–409.
18. McAllister, A. K. & Stevens, C. F. (2000) *Proc. Natl. Acad. Sci. USA* **97,** 6173–6178.
19. Mainen, Z. F., Malinow, R. & Svoboda, K. (1999) *Nature* **399,** 151–155.
20. Korn, H. & Faber, D. S. (1991) *Trends Neurosci.* **14,** 439–445.
21. Raastad, M., Storm, J. F. & Andersen, P. (1992) *Eur. J. Neurosci.* **4,** 113–117.
22. Bolshakov, V. Y. & Siegelbaum, S. A. (1995) *Science* **269,** 1730–1734.
23. Hanse, E. & Gustafsson, B. (2001) *J. Physiol.* **531,** 467–480.
24. Oertner, T. G., Sabatini, B. L., Nimchinsky, E. A. & Svoboda, K. (2002) *Nat. Neurosci.* **5,** 657–664.
25. Conti, R. & Lisman, J. (2003) *Proc. Natl. Acad. Sci. USA* **100,** 4885–4890.
26. Bekkers, J. M. & Stevens, C. F. (1991) *Proc. Natl. Acad. Sci. USA* **88,** 7834–7838.
27. Ryan, T. A., Reuter, H., Wendland, B., Schweizer, F. E., Tsien, R. W. & Smith, S. J. (1993) *Neuron* **11,** 713–724.
28. Liu, G. S. & Tsien, R. W. (1995) *Nature* **375,** 404–408.
29. Kirischuk, S., Veselovsky, N. & Grantyn, R. (1999) *Proc. Natl. Acad. Sci. USA* **96,** 7520–7525.
30. Forti, L., Bossi, M., Bergamaschi, A., Villa, A. & Malgaroli, A. (1997) *Nature* **388,** 874–878.
31. Tong, G. & Jahr, C. E. (1994) *Neuron* **12,** 51–59.
32. Wadiche, J. I. & Jahr, C. E. (2001) *Neuron* **32,** 301–313.
33. Hjelmstad, G. O., Isaac, J. T., Nicoll, R. A. & Malenka, R. C. (1999) *J. Neurophysiol.* **81,** 3096–3099.
34. Auger, C. & Marty, A. (2000) *J. Physiol.* **526,** 3–11.
35. Schikorski, T. & Stevens, C. F. (1997) *J. Neurosci.* **17,** 5858–5867.
36. Meyer, A. C., Neher, E. & Schneggenburger, R. (2001) *J. Neurosci.* **21,** 7889–7900.
37. Franks, K. M., Stevens, C. F. & Sejnowski, T. J. (2003) *J. Neurosci.* **23,** 3186–3195.
38. Scepek, S., Coorssen, J. R. & Lindau, M. (1998) *EMBO J.* **17,** 4340–4345.